Synergistic Antimicrobial Effects of Polyaniline Combined with Silver Nanoparticles

Qingming Jia,[1,2] Shaoyun Shan,[1] Lihong Jiang,[1] Yaming Wang,[1] Dan Li[1]

[1]*Faculty of Chemical Engineering, Kunming University of Science and Technology, Kunming 650224, China*
[2]*Faculty of Environmental Science and Technology, Kunming University of Science and Technology, Kunming 650093, China*

Received 19 June 2010; accepted 29 September 2011
DOI 10.1002/app.36257
Published online in Wiley Online Library (wileyonlinelibrary.com).

ABSTRACT: Silver/polyaniline nanocomposites (Ag NPs/PANI) containing PANI nanofiber and Ag nanoparticles were synthesized by one-step approach without using any extra reducing agent or surfactant and applied to new antimicrobial agents. Morphologies and crystallinity of the nanocomposites were characterized with SEM and XRD. The results showed that the average diameter of the PANI nanofibers is around 50–150 nm, and the average particle size of Ag NPs is around 100 nm. The crystallinity of PANI gets better with increasing silver nitride concentration. UV–vis absorption spectroscopy analysis indicated that the Ag NPs have some effect on the microstructure of PANI. The antimicrobial properties of Ag NPs/PANI against Gram-negative *Escherichia coli*, Gram-positive *Staphylococcus aureus* and fungous Yeast were evaluated using viable cell counts. The test results demonstrated that Ag NPs/PANI have enhanced antimicrobial efficacy compared to that of pure Ag NPs or pure PANI under the same test condition. The mechanism of the synergistic antimicrobial effect of Ag NPs with PANI was also proposed. In addition, thermal gravity analysis indicated that pure PANI and Ag NPs/PANI exhibit better thermal stability. © 2012 Wiley Periodicals, Inc. J Appl Polym Sci 000: 000–000, 2012

Key words: polyaniline; silver; antimicrobial properties; morphologies

INTRODUCTION

The increasing demands for better living environments have stimulated the development of consumer products with antimicrobial properties. Several new antibacterial and antifungal agents have been introduced recently,[1] whereas such new materials still have to fulfill the rather stringent requirements for real applications. Silver has been used for their antimicrobial activity, because the age of ancient Egyptians, and it has been proven antimicrobial agent with little hazardous side effects to mammalian cells.[2,3] However, the high cost and the difficulty to process into consumer products have limited its widespread uses. Silver nanoparticle (Ag NP) as an antimicrobial agent was observed already at low concentrations (units of milligrams per liter), which leads to a recent rapid development in the field of synthesis of the Ag NPs conveying the antimicrobial activity.[4,5] The performed research has proven that antimicrobial activity of the Ag NPs is dependent not only on their size but also on their shape.[6,7] The use of Ag NPs relieves the cost pressure to some extent and increases the antimicrobial efficiency due to the increased surface area,[8] but the processing problems such as intricate preparation process, easy aggregation, still remain. To overcome these problems, new methods of using metal oxide particles, diatomite, activated carbon, and polymers as carriers of Ag NPs have been developed.[9–13] However, it is necessary for these methods to reduce silver ions to Ag NPs by high temperature or adding various reductants. Therefore, preparing new antimicrobial agents that do not rely on reducing agents, structural directing molecules, or reduce process in high temperature is important.

Polyaniline (PANI) is a conducting polymer of particular interest, due its high stability, large conductivity range, low monomer cost, and the different redox states that can be obtained. More recently, metal/PANI composites have been investigated for several reasons. First, these nanocomposites are

Correspondence to: Y. Wang (wym@kmust.edu.cn).
Contract grant sponsor: National Natural Science Foundation of China; contract grant numbers: 50963004, 31160146.
Contract grant sponsor: China Postdoctoral Science Foundation; contract grant number: 20100471684.
Contract grant sponsor: Doctoral Fund of Ministry of Education of China; contract grant number: 20095314120003.
Contract grant sponsor: Project of Youth Academic Technology Personnel of Yunnan Province; contract grant number: 2009CI029.

expected to display several synergistic properties (e.g., catalysis,[14–16] sensors,[17–19] memory devices,[20] fuel cell,[21,22] and so on) between the PANI and the metal nanoparticles. Second, PANI possesses secondary amines and tertiary imines in the backbone structure that can bind metal ions, and the bound metal ions can be reduced by PANI to form zerovalent metals without using any reducing agent.[23,24] Third, the high surface to volume ratio of nanoparticles in these composites should result in a large number of binding sites available for chemical sensing or catalysis. Although applications of metal/PANI composites are imminent in many fields and some reports demonstrate that PANI is better biocompatible,[25,26] to the best of our knowledge, there is no report of investigation on the antimicrobial property of Ag NPs/PANI nanocomposites.

In the present work, a straightforward one-step approach is described for the synthesis of silver NPs-PANI nanofibers antimicrobial agent (Ag NPs/PANI) without using any extra reducing agent, surfactant, and/or large amounts of insoluble templates, and the synergistic antimicrobial effects of Ag NPs and PANI nanofibers on three types of bacteria, such as Gram-negative *Escherichia coli*, Gram-positive *Staphylococcus aureus*, and fungous Yeast, were illustrated.

EXPERIMENTAL

Materials

Aniline (AN), silver nitride, and ammonium peroxydisulfate are analytical purity grade and were purchased from Aladdin-reagent Co., Shanghai, China. Gram-negative *E. coli* (ATCC 8099), Gram-positive *S. aureus* (ATCC 6538), and fungous Yeast were purchased from Biocon Co., Japan and taken to investigate antimicrobial activity of Ag NPs/PANI nanocomposites. Luria–Bertani culture medium was purchased from Canspec Co., Shanghai, China.

Synthesis of Ag NPs/PANI nanocomposites

The Ag NPs/PANI nanocomposites with different silver contents were synthesized using nitric acid as follows. In a typical procedure for the preparation of Ag NPs/PANI nanocomposites, 2 mL (22 mmol) of AN monomer and quantitative silver nitride were dissolved in 200 mL of 1.0*M* nitric acid, and the mixture was put in a beaker. Then, 1.8 g of ammonium peroxydisulfate was dissolved in other beaker containing 200 mL of 1.0*M* nitric acid. The prepared solutions were then poured rapidly into a 1000-mL glass beaker and kept static conditions for 12 h at room temperature ($\sim$ 25°C), The product was filtered and washed with deionized water and ethanol for several times. The dark green powders were obtained after drying at room temperature for 24 h. The silver nitride content was varied from 0.0 to 4.4 mmol to investigate its effects on morphologies and antimicrobial property of PANI. These samples were marked as pure PANI (silver nitride content is 0.0 mmol), Ag NPs/PANI-50 (silver nitride content is 0.44 mmol, AN/Ag = 50), Ag NPs/PANI-10 (silver nitride content is 2.2 mmol, AN/Ag = 10), Ag NPs/PANI-5 (silver nitride content is 4.4 mmol, AN/Ag = 5), respectively. Using the ratio of AN and silver nitride weight to nanocomposites weight denotes yields of the nanocomposites, and the yields are about 87%.

For the purpose of comparison, the corresponding Ag NPs were synthesized by the reduction of the complex cation $[Ag(NH_3)_2]^+$ with D-maltose, as referred.[27]

Characterization

The morphologies of the resultant Ag NPs/PANI nanocomposites with different Ag contents were characterized by field-emission scanning electron microscopy (Philips XL 30). Before SEM imaging, the samples were not sputtered with thin layers of gold. The molecular structures of PANI were measured by UV–vis spectroscopy (TU-1901, Beijing Purkinje General Instrument Co.) and X-ray diffraction (XRD, Rigaku, D/Max 2400).

The antimicrobial activity was tested using the method of viable cell counts. First of all, Luria–Bertani culture medium was collocated for bacterial. Briefly, *E. coli*, *S. aureus*, or Yeast (about 10^5 CFU/mL) and 1 mg of pure Ag NPs, pure PANI, or Ag NPs/PANI nanocomposites were added to 100 mL the culture medium in the Erlenmeyer flask shaking in thermostat shaker at rate of 200 rps. About 0.1 mL so-made bacterial-prepared particles mixture was diluted with 0.9 mL the culture medium. Buffer solution (phosphate-buffered saline) and the culture medium containing prepared particles were completely mixed by vortex. No prepared particles were added to one Erlenmeyer flask containing 100 mL culture medium, which was served as a control sample. Subsequently, the bacterial suspension was diluted 10^4 times. One additional plate was poured containing 10 mL of nutrient agar for control purposes. The plates were incubated for 24 h at 37°C and then analyzed for the number of bacterial colonies to determine the growth inhibition rates of Ag/PANI composites in accordance with the eq. (1).

$$R(\%) = \frac{A - B}{A} \times 100 \quad (1)$$

where R defines the growth inhibition rates, A is the number of bacterial colonies from control sample,

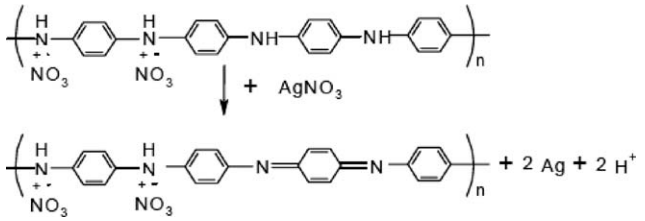

Scheme 1 Chemical reaction between PANI and silver ions.

and *B* is the number of bacterial colonies from pure Ag NPs, pure PANI, or Ag/PANI nanocomposites.

Thermogravimetric analysis (TGA) thermograms were obtained on a STA 449F3 instruments equipment (NETZSCH Co., Germany), under nitrogen atmosphere at a heating rate 10°C/min, and scanned from room temperature to 1000°C. The samples ranged between 15 and 25 mg in weight and were placed in platinum sample pans under a continuous nitrogen flow 100 mL/min.

RESULTS AND DISCUSSION

SEM analysis

The generation of silver *in situ*, by the reduction of silver ions with PANI, is a feasible approach.[28] PANI alone,[29] PANI colloids,[30] and PANI deposited on cellulose fibres[31] have all been used as reductants of silver nitrate. PANI protonated with nitric acid is oxidized with silver nitrate and reduced units o f PANI supply protons to reduce Ag(1), and each PANI repeating unit can convert two single charged metal ions into two metal atoms. The redox process can be showed by the Scheme 1. The morphologies of the pure PANI and Ag NPs/PANI nanocomposites were shown in Figure 1. Figure 1(a) indicates that the pure PANI consists of nanofibers with diameter around 50 nm, and the length of the fibers ranges from hundreds of nanometers to several micrometers. But, it is observed that some aggregations exist in the pure PANI. When Ag ion is added into reaction system, the resultant Ag NPs/PANI nanocomposites consist of uniform nanofibers and spherical Ag nanoparticles, as shown in Figure 1(b–d). In addition, it is observed that many fibers join with others and form branched structures or interconnected networks in Ag NPs/PANI nanocomposites. Comparing Figure 1(b) with Figure 1(c) or Figure 1(d), one can see that the diameter of the PANI nanofibers increases, and the diameter of Ag nanoparticles increases with Ag loading content increase. The size of the Ag nanoparticles (bright regions) could be varied with changing the AN/metal salt ratio. Typically, when spherical Ag particles with diameters of around 100 nm form at high Ag concentration (AN/Ag = 5). The above results reveal that Ag ion concentration affects not only morphology of PANI, but also size of Ag nanoparticles. For the purpose of comparison, the corresponding Ag NPs were synthesized by the reduction of the complex cation $[Ag(NH_3)_2]^+$ with D-maltose [as shown Fig. 1(e)], and the diameter of the spherical Ag particles is about 200 nm.

XRD analysis

Figure 2 shows XRD spectra of the pure PANI and Ag NPs/PANI nanocomposites with different Ag contents. As can be seen from Figure 2, the XRD spectra of Ag NPs/PANI nanocomposites show that these diffraction features appear at about 38.1°, 44.1°, 64.4°, and 77.3°, corresponding to the (111), (200), (220), and (311) planes of the cubic phase of Ag, respectively.[32] The size *D* of the Ag particles can be given by Scherrer's equation:

$$D = \frac{0.89\lambda}{\beta \cos\theta} \quad (2)$$

where λ is the X-ray wavelength, β is the half-height width of the XRD peak, and θ is the Bragg angle. According to the β values of the Ag(111) and Ag (220) peaks, using eq. (2), the Ag particle size in PAN/Ag (molar ratio of AN and Ag is 5 : 1) is calculated to be about 100 nm. The result means that the Ag in the PANI/Ag powder has a nanoparticle size. The symbol *a* in Figure 2 may be diffraction peaks of the cube Ag_2O (111).

Significant differences in XRD between the Ag NPs/PANI nanocomposites and pure PANI were also observed as shown in Figure 2 (indicated a black arrow). As one can see, one sharp peak at $2\theta = 6.34°$, which can be assigned as the periodic distance between the dopant and N atom on adjacent main chains,[33,34] is observed for the Ag NPs/PANI nanocomposites. Moreover, intensity of the peak becomes stronger and stronger with increasing Ag loading content, indicating short-range order of the counter-ions along the polymer chain of the PANI/Ag. In addition, the two broad bands centered at $2\theta = 19.7°$ and $2\theta = 25.1°$, which are ascribed to the periodicity parallel and perpendicular to the polymer chains of PANI, respectively, are observed in the pure PANI and Ag NPs/PANI nanocomposites. However, the two bands become stronger with Ag loading content increase. Especially, when the molar ratio of AN and Ag is up to 5 : 1, there are two obvious bands at $2\theta = 19.7°$ and $2\theta = 25.1°$. The above results indicate that adding Ag into PANI makes the crystallinity of PANI high. The phenomenon may be explained by

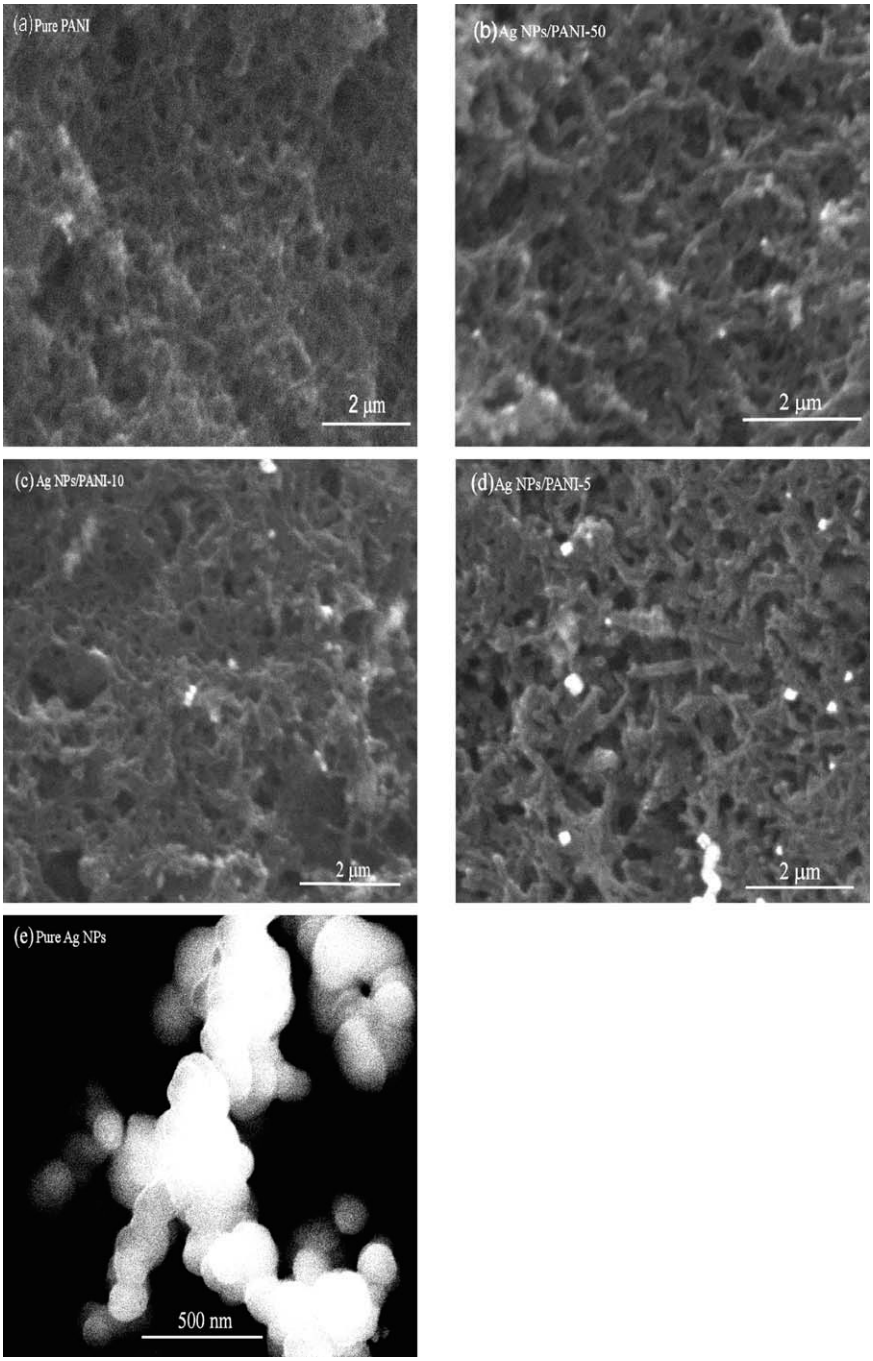

Figure 1 SEM images of the different pure Ag and Ag NPs/PANI nanocomposites.

the following reasons. The polymerization rate is faster with increasing silver nitride content, and this is indirectly observed through rapid color change of reaction medium from transparent to dark green color. Because the fast polymerization shortens the growth time of PANI, the crystallinity of PANI is high without undesired shapes. Besides catalytic effect of Ag ion on accelerating AN polymerization, this phenomenon may be attributed to the number increase of available reaction sites on the polymer chain with decreasing Ag(1)/N molar ratio.

UV–vis absorption spectroscopy analysis

UV–vis absorption spectra of pure PANI, Ag NPs/PANI nanocomposites are shown in Figure 3. The characteristic peaks of the pure PANI and Ag NPs/PANI nanocomposites appear at 302, 420, and 836 nm, which are attributed to π–π*, polaron–π*, and π–polaron transitions, respectively.[35] The results suggest that the prepared PANI and Ag NPs/PANI nanocomposites are in a doped state.

Ag NPs show a maximum absorption peak at about 400 nm corresponding to a surface plasmon

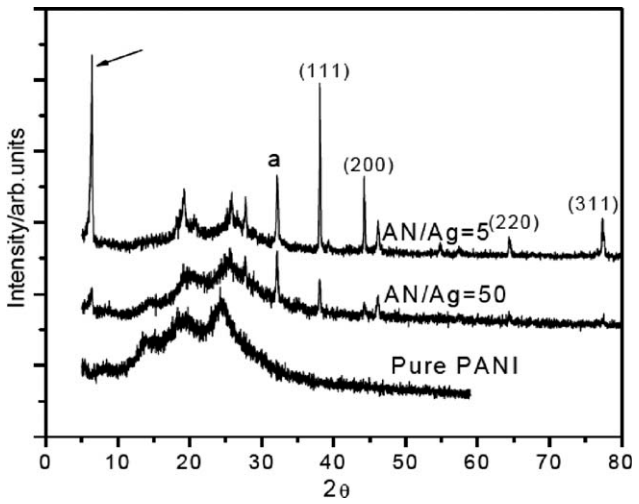

Figure 2 XRD spectra of Ag NPs/PANI nanocomposites.

resonance due to the transverse oscillation of electrons along the nanoparticles.[36] This overlaps with the absorption band of PANI, and so it is difficult to differentiate them. It clearly shows from Figure 3 that the bands at 400–420 nm due to the benzenoid rings of the PANI are overlapped, and the position of the absorption maximum is blue-shifted due to the presence of Ag nanoparticles, which indicates that the Ag NPs/PANI nanocomposites have a different electronic environment than the pure PANI. The absorption peak about 420 nm in the UV–vis curves of Ag NPs/PANI nanocomposites is sharp, indicating the Ag particles size distribution is quite narrow.[37] Moreover, the absorption peak is stronger, but the blue-shift of this peak is not obvious with increasing the silver ions concentration, which proves that the numbers of Ag particles increase and the diameter of Ag particles changes a little. Figure 3 also shows that the absorption peak of the π–polaron transitions is broader and shifts to a higher wavelength in the Ag NPs/PANI nanocomposites, compared to that of the pure PANI. This result indicates that the doping level is higher, and the as-prepared PANI is more delocalized in the Ag NPs/PANI nanocomposites than in pure PANI. This higher doping level also indicates that quinoid phenyl rings, and the oxidized units of PANI increase with silver ions concentration.

Antimicrobial activity analysis

The antimicrobial activity study of Ag NPs/PANI nanocomposites was carried out against Yeast, Gram-positive *S. aureus*, and Gram-negative *E. coli* by using Ag NPs/PANI nanocomposites with different Ag NPs contents. A photograph of colony-forming units versus Ag content for Yeast was constructed (Fig. 4) to visualize the inhibition rates. Figure 4 shows that the pure Ag particles and pure PANI have some antimicrobial activity against Yeast, and the colony-forming units decreases more rapidly with the Ag content increase in Ag NPs/PANI nanocomposites.

Table I summarizes the results obtained for growth inhibition rates (R) of the pure Ag particles, pure PANI, and Ag NPs/PANI nanocomposites with different Ag contents against Yeast, *S. aureus*, and *E. coli*. Comparing the experimental results in Table I, we notice that the pure Ag particles and pure PANI have some antimicrobial activity against Yeast, *S. aureus*, and *E. coli*, and the pure Ag particles are more effective in killing *S. aureus*, but the pure PANI are more effective in killing *E. coli*. Meanwhile, it can be seen from Table I that R of test bacteria also increases with the Ag content increase in Ag NPs/PANI nanocomposites, which indicates some synergistic antimicrobial effects of PANI combined with Ag NPs. Especially, the R of *S. aureus* is 99.9%, when the mole ratio of AN and silver ion in Ag NPs/PANI nanocomposites is 10.

To explain the mechanism of the synergistic antimicrobial effect of Ag NPs/PANI nanocomposites, in combination with the previous results, we present the hypothesis as follows.

On one hand, the synergistic effect may be caused by interactions between Ag NPs and PANI, which formed during preparing Ag NPs/PANI nanocomposites and changed the structures and morphologies of pure PANI or Ag. PANI is effective in stabilizing particles against aggregation in the Ag NPs/PANI nanocomposites. Ag NPs create redox imbalance causing extensive bacterial death, and smaller Ag NPs having the large surface area would give more bactericidal effect than the larger Ag NPs.[38] Meanwhile, SEM and UV–vis absorption spectroscopy analysis proved that Ag ions have obvious effect on the morphologies and electronic

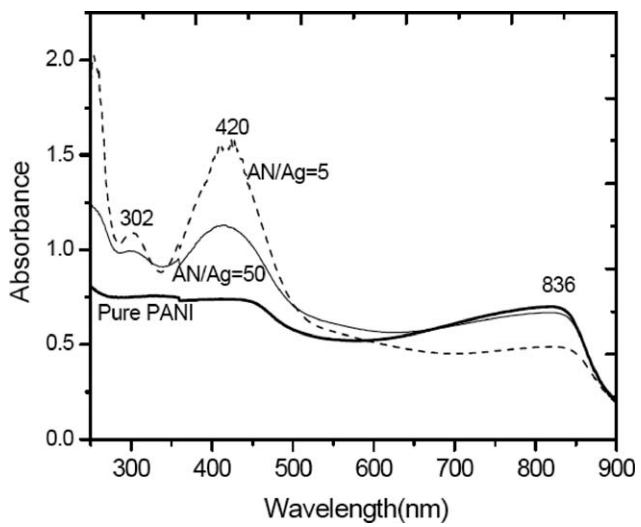

Figure 3 UV–vis absorption spectra of Ag NPs/PANI nanocomposites.

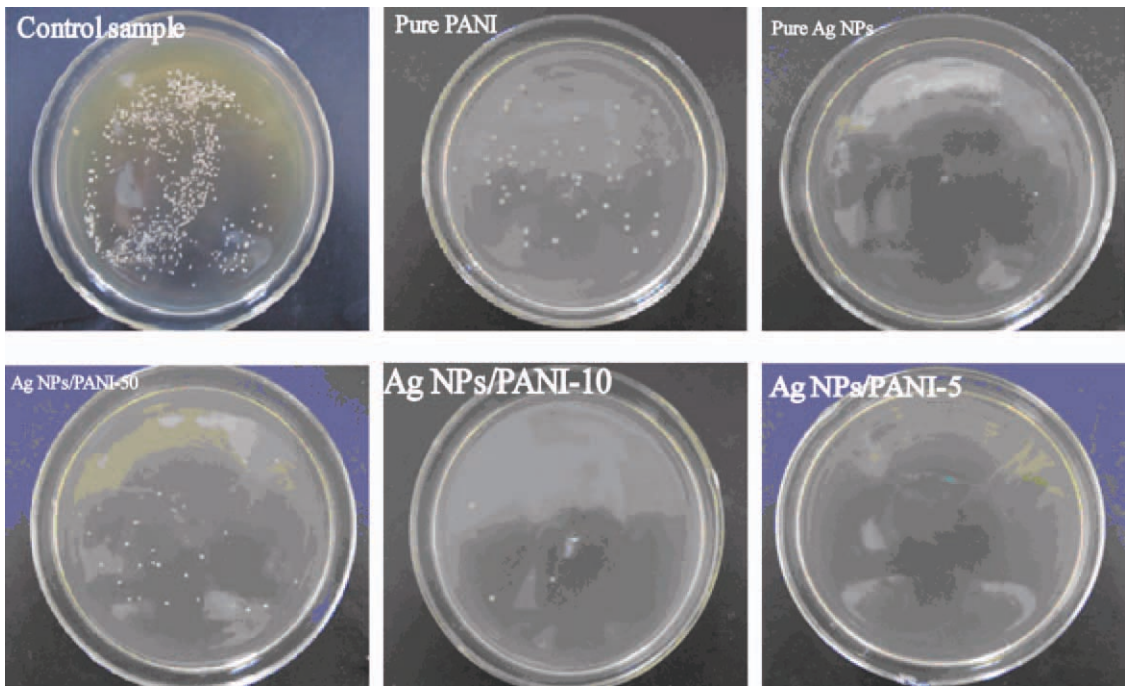

Figure 4 Photographs of the test plates with Yeast colonies in the presence of the different antibacterial agents. [Color figure can be viewed in the online issue, which is available at wileyonlinelibrary.com.]

environment of PANI, which benefits enhancing antimicrobial properties. On the other hand, a more probable cause of the synergistic effect may be the different cell wall composition of the different types of bacteria. For example, Yeast cell wall composes of cellulose. *S. aureus* is Gram-positive (G^+) bacteria, and the cells form a negatively charged environment. Ag ions with a positive charge from Ag NPs surface will be more negatively charged surface of *S. aureus* adsorbed to the surface. However, *E. coli* is Gram-negative (G^-) bacteria, the cell wall as a multilayer structure, making the cell wall with low-osmotic pressure, which facilitates contacting PANI molecules and the cell wall of *E. coli*.

Thermal gravity analysis

The thermal stability of Ag NPs/PANI nanocomposites with different Ag contents was tested by the thermogravimetric analysis (TGA), and the results are plotted in Figure 5. As shown in Figure 5, The decomposed process consists of a two-stage degradation: the early stage with a maximum rate at about 250°C, assigned to the thermal degradation of nitric acid, and the second stage with a maximum rate at about 460°C, assigned to the thermal degradation of PANI molecules, which indicates that the Ag NPs/PANI nanocomposites have better thermal stability. Moreover, the weight loss decreases with increasing Ag content.

TABLE I
Growth Inhibition Rates of Ag NPs/PANI Nanocomposites Against Yeast, *S. aureus*, and *E. coli*

Test samples	Growth inhibition rates (R, %) of test bacteria		
	Yeast	*S. aureus*	*E. coli*
Pure Ag particles	79.4 ± 0.9	90.0 ± 0.6	70.7 ± 0.5
Pure PANI	73.8 ± 0.3	72.5 ± 0.5	82.6 ± 0.7
Ag NPs/PANI-50	89.0 ± 0.8	90.6 ± 0.9	86.9 ± 0.8
Ag NPs/PANI-10	95.9 ± 0.4	99.9	92.9 ± 1.0
Ag NPs/PANI-5	99.9	99.9	99.9

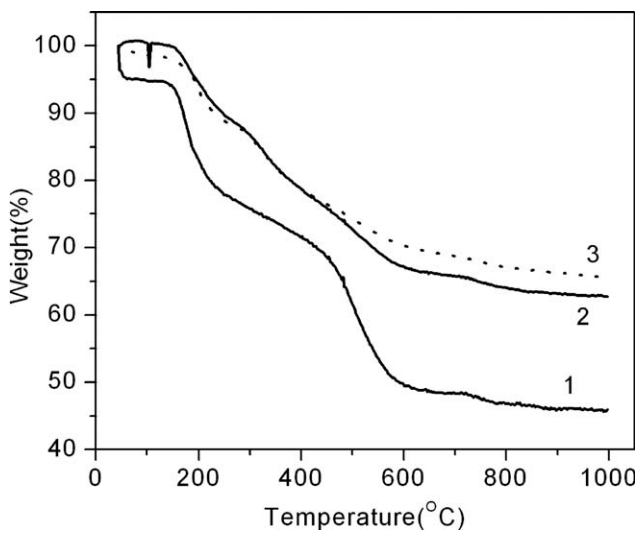

Figure 5 TG curves of Ag NPs/PANI nanocomposites.

CONCLUSIONS

It is concluded from this study that Ag NPs/PANI nanocomposites were synthesized by one-step approach without using any reducing agent. SEM and XRD analysis results showed that the average diameter of the PANI nanofibers was around 50–150 nm, and the average particle size of Ag NPs was around 100 nm. The crystallinity of PANI gets better with increasing silver nitride concentration. The combination of Ag NPs and PANI has a synergistic antimicrobial efficiency on *E. coli*, *S. aureus*, and Yeast bacteria. We present a hypothesis to explain the antimicrobial mechanism. This research, though very preliminary, provides helpful insights to the development of novel antimicrobial agents. To elucidate the mechanism of this synergistic antimicrobial effect, it is necessary to perform more elaborate experimental evidences.

References

1. Ray, S.; Mohan, R.; Singh, J. K.; Samantaray, M. K.; Shaikh, M. M.; Panda, D.; Ghosh, P. J Am Chem Soc 2007, 129, 15042.
2. Ho, C. H.; Tobis, J.; Sprich, C.; Thomann, R.; Tiller, J. C. Adv Mater 2004, 16, 957.
3. Lee, D.; Cohen, R. E.; Rubner, M. F. Langmuir 2005, 21, 9651.
4. Morones, J. R.; Elechiguerra, J. L.; Camacho, A.; Holt, K.; Kouri, J. B.; Ramirez, J. T.; Yacaman, M. J. Nanotechnology 2005, 16, 2346.
5. Panacek, A.; Kvitek, L.; Prucek, R.; Kolar, M.; Vecerova, R.; Pizurova, N.; Sharma, V. K.; Nevecna, T.; Zboril, R. J Phys Chem B 2006, 110, 16248.
6. Sotiriou, G. A.; Pratsinis, S. E. Environ Sci Technol 2010, 44, 5649.
7. Liu, J.; Sonshine, D. A.; Shervani, S.; Hurt, R. H. ACS Nano 2010, 4, 6903.
8. Melaiye, A.; Sun, Z.; Hindi, K.; Milsted, A.; Ely, D.; Reneker, D.; Tessier, C. A.; Youngs, W. J Am Chem Soc 2005, 127, 2285.
9. Amin, S. A.; Pazouki, M.; Hosseinnia, A. Powder Technol 2009, 196, 241.
10. Su, W.; Wei, S. S.; Hu, S. Q.; Tang, J. X. J Hazard Mater 2009, 172, 716.
11. Wang, X. S.; Wang, H.; Coombs, N.; Winnik, M. A.; Manners, I. J Am Chem Soc 2005, 127, 8924.
12. Porel, S.; Singh, S.; Harsha, S. S.; Rao, D. N.; Radhakrishnan, T. P. Chem Mater 2005, 17, 9.
13. Chauhan, B. P. S.; Sardar, R. Macromolecules 2004, 37, 5136.
14. Santhosh, P.; Gopalan, A.; Lee, K. P. J Catal 2006, 238, 177.
15. Amaya, T.; Saiom, D.; Hirao, T. Tetrahedron Lett 2007, 48, 2729.
16. Houdayer, A.; Schneider, R.; Billaud, D.; Ghanbaja, J.; Lambert, J. Appl Organomet Chem 2005, 19, 1239.
17. Wanekaya, A. K.; Chen, W.; Myung, N. V.; Mulchandani, A. Electroanalysis 2006, 18, 533.
18. Feng, X.; Mao, C.; Yang, G.; Hou, W.; Zhu, J. J. Langmuir 2006, 22, 4384.
19. Langer, J. J.; Filipiak, M.; Kecinska, J.; Jasnowska, J.; Wlodarczak, J.; Buladowski, B. Surf Sci 2004, 573, 140.
20. Tseng, R. J.; Baker, C. O.; Shedd, B.; Huang, J.; Kaner, R. B.; Ouyang, J.; Yang, Y. Appl Phys Lett 2007, 90, 053101.
21. Yang, Y.; Ouyang, J.; Ma, L.; Tseng, R. J. H.; Chu, C. W. Adv Funct Mater 2006, 16, 1001.
22. Chen, Z.; Xu, L.; Li, W.; Wa, M.; Yan, Y. Nanotechnology 2006, 17, 5254.
23. Smith, J. A.; Josowicz, M.; Janata, J. Phys Chem Chem Phys 2005, 7, 3614.
24. Smith, J. A.; Josowicz, M.; Janata, J. J Electrochem Soc 2003, 150, E384.
25. Li, M. Y.; Guo, Y.; Wei, Y.; MacDiarmid, A. G.; Lelkes, P. I. Biomaterials 2006, 27, 2705.
26. Bidez, P. R.; Li, S.; MacDiarmid, A. G.; Venancio, E. C.; Wei, Y.; Lelkes, P. I. J Biomater Sci Polym 2006, 17, 199.
27. Kvitek, L.; Prucek, R.; Panacek, A.; Novotny, R.; Hrbac, J.; Zboril, R. J Mater Chem 2005, 15, 1099.
28. Tsakova, V. J Solid State Electrochem 2008, 12, 1421.
29. Stejskal, J.; Prokeš, J.; Sapurina, I. Mater Lett 2009, 63, 709.
30. Li, W. G.; Jia, Q. X.; Wang, H. L. Polymer 2006, 47, 23.
31. Kelly, F. M.; Johnston, J. H.; Borrmann, T.; Richardson, M. J. Eur J Inorg Chem 2007, 2007, 5571.
32. Sun, Y. G.; Yin, Y. D.; Mayers, B. T.; Herricks, T.; Xia, Y. N. Chem Mater 2002, 14, 4736.
33. Yang, Y.; Wan, M. J Mater Chem 2002, 12, 897.
34. Zhang, L.; Wan, M. Adv Funct Mater 2003, 13, 815.
35. Xia, H. S.; Wang, Q. Chem Mater 2002, 14, 2158.
36. Caswell, K. K.; Bender, C. M.; Murphy, C. J. Nano Lett 2003, 3/5, 667.
37. Khanna, P. K.; Singh, N.; Charan, S.; Viswanath, A. K. Mater Chem Phys 2005, 92, 214.
38. Shah, M. S. A. S.; Nag, M.; Kalagara, T.; Singh, S.; Manorama, S. V. Chem Mater 2008, 20, 2455.